Physica E 41 (2009) 1029–1033

Contents lists available at ScienceDirect

Physica E

journal homepage: www.elsevier.com/locate/physe

Assessment of the main material issues for achieving an Er coupled to silicon nanoclusters infrared amplifier

D. Navarro-Urrios [a,*], A. Pitanti [a], N. Daldosso [a], F. Gourbilleau [b], L. Khomenkova [b], R. Rizk [b], L. Pavesi [a]

[a] Laboratorio di Nanoscienze, Dipartimento di Fisica, Università di Trento, Via Sommarive 14, I-38050 Povo (Trento), Italy
[b] CIMAP, UMR CNRS 6252, CEA/CNRS/Ensicaen/Université de Caen 6 Boulevard Maréchal Juin, 14050 Caen, France

ARTICLE INFO

Available online 20 August 2008

PACS:
78.55.−m
78.66.−w
81.15.Gh

Keywords:
Silicon nanoclusters
Erbium
Optical amplifier
Silicon photonics
Waveguides

ABSTRACT

In this work we present the state of the art of our work to obtain an infrared optical amplifier in which Er^{3+} doped SiO_2 sensitised with Si nanoclusters (Si-nc) act as the active material to provide the signal amplification. As a result of a careful optimisation of the deposition parameters we have achieved that the Er^{3+} fraction coupled with the Si-nc with respect to the total optically active Er^{3+} content is about 23%. This result has been determined both by quantitative measurements of the first excited state population and by pump and probe amplification measurements under non-resonant pumping, where 1 dB cm^{-1} of internal gain (reduction of 2 dB cm^{-1} of the initial absorption losses) has been obtained.

We will discuss several material issues that are mandatory to address and then overcome in order to optimise the fraction of Er^{3+} coupled to Si-nc, with the aim of exciting all the ions through indirect transfer. In particular we will address: carrier absorption (CA) in Si-nc, cooperative up-conversion and non-radiative recombination in Er^{3+}, together with the distance dependent interaction and Auger back-transfer processes in the Er/Si-nc coupled system.

1. Introduction

Integrated erbium-doped waveguide amplifiers (EDWAs) are fundamental elements in planar lightwave circuits thank to their compactness and easy of integration on silicon wafers. However, a limitation to their wide use is their cost and footprint. One way to overcome these restrictions is by using the broad-band efficient sensitisers for Er^{3+} ions such as Si nanoclusters (Si-nc) in SiO_2 which could allow substituting expensive pump laser sources by low cost broad-band excitation lamps [1]. Sensitisation is demonstrated by the enhancement of the effective excitation cross section of the Er^{3+} 1.54 μm luminescence (σ_{eff}), which broadens and strengthens up to values of about 10^{-16} cm^2, when low pump flux visible light is used [1–6].

The most general requirement for realising an optical amplifier is to have an active material that can provide an optical gain which is high enough to compensate the passive losses (propagation and coupling losses) of the waveguides. In a recent work [7], we have demonstrated that Er/Si-nc active waveguides show propagation losses at 1600 nm as low as 2.6 dB cm^{-1} and confinement factors as high as 70–80% at 1.54 μm. In addition, we have measured absorption losses at the absorption peak or Er^{3+} ($\lambda = 1535$ nm) from 4 to 6 dB cm^{-1}. Hence, if we would invert the whole population, net optical gain would be achieved, which is highly challenging if realised by using a low cost and low power optical pump. This can be demonstrated once the Si-nc to Er^{3+} coupling is optimised such that the whole optically active Er^{3+} population is excited through indirect transfer from the Si-nc. However, in the last years the expectations generated on this material have decreased after the publication of several reports revealing what seemed to be an intrinsic limit of the material itself. In fact, previous studies suggest that only few percents (i.e., from 0.5% to 3%) of the optically active Er^{3+} population are susceptible to be excited through energy transfer from the excitons generated within the Si-nc [7–11].

The aim of this article is to address the main material issues for samples of Er^{3+} doped SiO_2 sensitised with Si-nc produced by reactive magnetron co-sputtering samples. Indeed, there are many processes that can compete with the transfer mechanism between Si-nc and Er^{3+}, generating extra pump power dependent losses or increasing the pump threshold necessary for Er^{3+} ions population inversion. First, there are competitive processes that increase the exciton recombination rate, like Auger processes within a Si-nc. Second, carrier absorption (CA) phenomena within the Si-nc can lead to an induced signal absorption. Third, non-radiative recombinations and, in particular, cooperative up-conversion between excited Er^{3+} can rise dramatically the pump threshold which is necessary to obtain population inversion even though the Er^{3+}/Si-nc transfer is optimised. The most difficult aspect is the optimisation

* Corresponding author.
E-mail address: dnavarro@el.ub.es (D. Navarro-Urrios).

1386-9477/$ - see front matter © 2008 Elsevier B.V. All rights reserved.
doi:10.1016/j.physe.2008.08.030

of the Er^{3+}/Si-nc coupling rate. The dependence of the transfer rate on the distance between Er^{3+} and the Si-nc makes Er^{3+} far from the Si-nc so that it cannot benefit from the enhancement of the effective excitation cross section and, thus, can only be excited directly, which in turn reduce the coupled Er^{3+} content. On the contrary, some reports have suggested that not the distance dependent interaction but Auger back transfer is the most severe limitation to the application of this material [12,13]. Auger back transfer is a process by which excitation is back transferred from Er^{3+} to Si-nc. This implies that it would be possible to have even 100% Er^{3+} coupled to Si-nc, but most of it would relax non-radiatively exciting the Si-nc. It was suggested that this process could only be eliminated by carefully engineering the Si-nc band structure, which is almost an impossible task when dealing, like in our case, with amorphous nanoclusters.

In this work, we demonstrate that, by carefully optimising the deposition and annealing conditions versus the mentioned detrimental processes, we have reached an Er^{3+}/Si-nc coupled content of 23% of the optically active Er^{3+} population. We also demonstrate that Auger back-transfer processes are not present in our samples and thus we propose a model in which the limited interaction distance between Si-nc and Er^{3+} ions is the restricting magnitude for the non-complete excitation of the whole Er^{3+} active population. We believe that these results re-launch the expectations of feasibility of an optical amplifier based on this material since the process of material optimisation becomes mainly a geometrical problem that can be solved by placing the Er^{3+} ions in regions closer to the Si-nc surface than Si-nc/Er^{3+} mean interaction distance.

2. Experimental

The layers investigated have been fabricated using an original approach of RF reactive magnetron sputtering of 2-in. confocal pure SiO_2 and Er_2O_3 targets under argon–hydrogen mixture. The ability of the reactive H_2 gas to reduce the oxygen–silicon species originating from the sputtered target was used to allow the incorporation of Si excess in the layers, as previously described [14]. The deposition was performed onto 2-in silicon substrates covered by stoichiometric thermal silica of 5-μm thickness. More details on sample preparation can be found elsewhere [14]. In this work we will examine a series of samples optimised in terms of high PL emission from Er^{3+} ions under non-resonant pumping and long Er^{3+} lifetime for the $^4I_{13/2} \rightarrow {}^4I_{15/2}$ transition (some milliseconds). We will report mainly on two samples labelled A (Si excess of 5% and Er^{3+} content of 3.4×10^{20} cm^{-3}) and C (Si excess of 8.5% and Er^{3+} content of $4 \times 10^{20}\,cm^{-3}$), sample C being our starting point prepared by reactive magnetron co-sputtering of a single target of pure silica topped with Er_2O_3 pellets.

Layer A has been fabricated with an applied RF power of 150 and 15 W on SiO_2 and Er_2O_3 cathodes, respectively, while the substrate temperature was fixed to 100 °C. The hydrogen and argon partial pressures were equal and the working pressure of the plasma was kept at 3 mTorr. The details of the fabrication of sample C has been previously described [15]. Both layers were annealed at 910 °C during 60 min in pure nitrogen flow.

Some of the measurements shown in this paper (mainly those related to CA characterisation) were done on rib-loaded waveguides, that have been formed by dry etching the slab waveguides. The etching depth and the channel widths have been chosen in order to optimise the confinement factor Γ of the guided mode and to realise a mono-modal optical waveguide.

3. Experimental results

3.1. CA on Si-nc

We have focused a large part of our efforts on the understanding and quantification of the CA mechanism within the Si-nc when a signal at about 1.54 μm is propagating. This process generates additional losses that are detrimental for the performances of devices based on this material, since the excitons photogenerated within the Si-nc due to absorption of pumping photons [16], they can absorb signal photons instead of recombining and then transfer them to the Er^{3+} ions. The absorbed energy is thus employed to bring the carriers to higher energetic states.

In the case of Si-nc coupled to erbium systems, CA could generate strong losses if the coupling with erbium ions is not efficient enough to strongly reduce the exciton lifetime.

The CA loss measurements shown in Fig. 1 have been performed on rib-waveguides by means of a pump and probe technique, reported elsewhere [16]. A signal light at 1.54 μm has been butt-coupled to the waveguides and the light exiting the end facet of the waveguide was measured by an IR detector. A top-pumping geometry was used where the pump light was provided by a 488 nm laser and was focused on the waveguide surface into a strip of 100 μm wide and 1 cm long by means of a cylindrical lens.

We have followed two strategies to decrease the CA. The first is to carefully decrease the size of the Si-nc (by means of the annealing time, being fixed all the optimised deposition parameters) as it is suggested in the top panel of Fig. 1. In this panel, it is shown that by decreasing the annealing time while maintaining the same Si-nc density, the CA losses decrease accordingly due to the reduction of the Si-nc size. The second is to increase the energy transfer probability. On one hand, it generates obvious benefits in terms of the material performance. On the other hand, it reduces the exciton lifetime, which in turn means a decreasing probability of having a CA process. To illustrate this, in the bottom panel we show the CA losses measured with two samples with the same Si-nc composition but with two different Er^{3+} concentrations. By increasing this concentration, the probability of exciton recombination due to an energy transfer also increases since we increased the quantity of Er^{3+} ions close enough to the Si-nc to be excited indirectly.

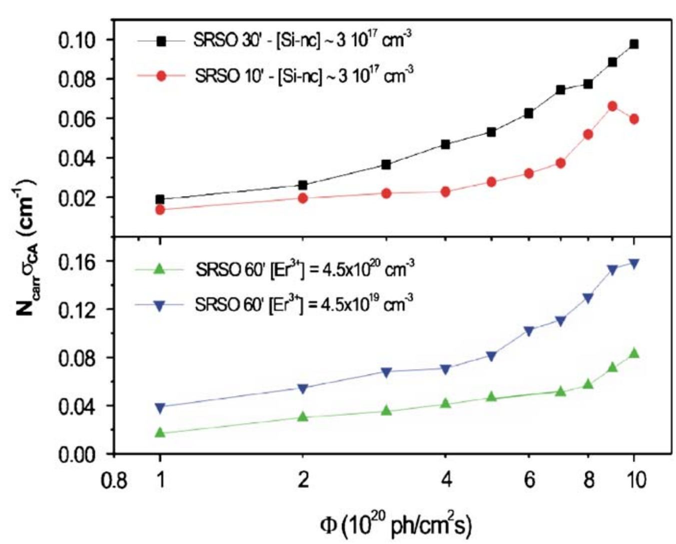

Fig. 1. Carrier absorption losses for two samples with the same Si-nc density but different annealing times (top panel) and for two samples with the same Si-nc composition but different Er^{3+} contents (bottom panel).

3.2. Cooperative up-conversion and total lifetime in Er^{3+}

One of the keys of the technologic success of erbium is that the $^4I_{13/2}$ level is well separated in energy from the fundamental level. This forces the recombination probability to be mainly radiative, and, because it is a parity forbidden transition, it shows a long lifetime (some milliseconds). This is a critical requirement for achieving population inversion with a reasonable pumping power. It is thus clear that it is very important to maximise the total lifetime of the transition by reducing the non-radiative decay probability, which is experimentally determined with time resolved PL measurements at 1.54 μm.

Among other non-radiative recombination paths, cooperative up-conversion recombination between closely excited Er^{3+} ion pairs has been thought to play an important role as a limiting process to obtain population inversion. In a cooperative up-conversion process, one of the two nearby interacting Er^{3+} ions, both in the first excited state, gives up resonantly and non-radiatively its energy to the other, collapsing to the ground state and bringing the other in the $^4I_{9/2}$ level.

The differential equation that rules the decay rate of the excited level of the Er^{3+} population (N_2) taking into account specifically the cooperative up-conversion is as follows:

$$\frac{dN_2(t)}{dt} = -\frac{N_2(t)}{\tau} - C_{up}N_2(t)^2 \quad (1)$$

where τ is the total lifetime, which counts for the radiative and the N_2 independent non-radiative recombination paths, and C_{up} is the up-conversion coefficient between pairs of excited ions.

As can be interpreted from the previous equation, at low pump fluxes (10^{16}–10^{17} photons $cm^{-2}\,s^{-1}$) the temporal decay of the PL signal is usually expected to be a single exponential function, which allows associating the behaviour of the non-radiative lifetime to recombinations with defects or to concentration quenching effects between excited and non-excited Er^{3+} ions. It is worth noting that the probability of having this kind of recombinations is independent of the excited Er^{3+} and, therefore, of the pump photon flux. By increasing the pump flux, cooperative up-conversion recombination between close excited Er^{3+} ion pairs could start to play an important role among the other non-radiative recombination paths because the concentration of Er^{3+} found in the first excited state increases accordingly.

In Fig. 2 we show the normalised PL decaying signal at two pump fluxes (pumping resonantly at 488 nm) which differs in more than two orders of magnitude. We report the results of samples A (solid squares and empty circles) and C (solid triangles and empty inverted triangles).

For sample C, the extracted total lifetime is about 3.8 ms and it is clear the role of up-conversion ($C_{up} = 2\times10^{-17}\,cm^3\,s^{-1}$) in stretching the exponential decay when rising the photon flux. Further information regarding the determination of C_{up} and τ on this sample by means quantitative measurements of the first excited state population can be found elsewhere [11].

However, for sample A, it can be seen that both decays are single exponential with a total lifetime of 5.5 ms. This value is remarkably long due to the strong reduction of non-radiative recombination mechanisms. Moreover, even though the initial N_2 is higher than in sample C for the same pump flux, cooperative up-conversion processes are negligible in this case.

3.3. Quantification of the optically active erbium ion concentration: distance dependent interaction in the Si-nc:Er^{3+} system

From standard rate equation approach, it can be demonstrated that the first excited state population N_2 is related to the photon flux through the following relation:

$$N_2 = N_{ac,Sinc}\frac{\sigma_{eff}\Phi}{\sigma_{eff}\Phi + 1/\tau} \quad (2)$$

where $N_{ac,Sinc}$ is the number of optically active Er^{3+} ions coupled to the Si-nc and Φ is the pump photon flux. To evaluate this number, both the effective excitation cross section (σ_{eff}) and Er^{3+} first excited state population (N_2) are needed.

σ_{eff} can be extracted from time resolved photoluminescence measurements. In fact, the difference between the reciprocals of the risetime (τ_r) and decay time (τ_d) can be related with the pump flux by the following equation:

$$\frac{1}{\tau_r} - \frac{1}{\tau_d} = \sigma_{eff}\Phi \quad (3)$$

In the inset of Fig. 3, we show the rise and decay time of the PL signal (1535 nm) for different pump fluxes in the case of sample A.

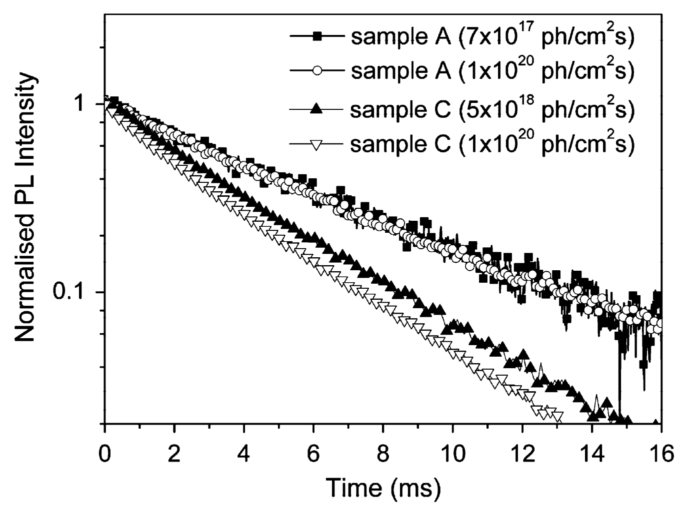

Fig. 2. Normalised PL decays in log scale for two different pump photon fluxes. The solid squares and empty circles correspond to sample A while the solid triangles and empty inverted triangles are associated to sample C.

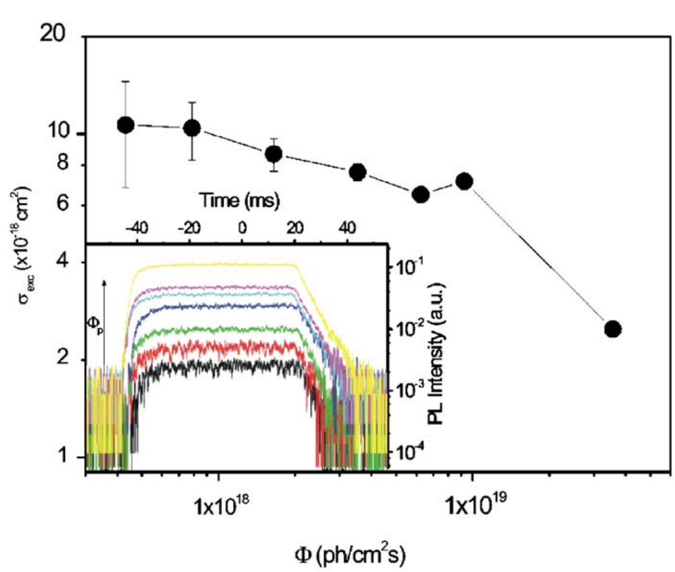

Fig. 3. Effective excitation cross section under non-resonant pumping (476 nm) as a function of the photon flux. The inset shows the rise and decay signal for different pump fluxes.

It is well known that the σ_{eff} under 476 nm excitation is depending on the photon flux, therefore it is necessary to determine it for every flux, what is shown in Fig. 3. σ_{eff} is indeed decreasing as a function of the photon flux. In several previous reports [10,11] we have demonstrated that Er^{3+} ions near the Si-nc are efficiently coupled to them, whereas Er^{3+} ions far away are uncoupled and behave as Er^{3+} in SiO_2 which can be excited only directly (which in the case of 476 nm pumping gives a negligible contribution to the PL). In accordance to this model, the slope change of σ_{eff} as a function of the photon flux (see Fig. 3) is thus explained in the following way: the closest Er^{3+} provide most of the PL signal at low fluxes and, therefore, the system has a very high σ_{eff}. Increasing the pump flux, the signal coming from the Er located far away from the Si-nc becomes more and more important which translates into a reduction of σ_{eff}.

To evaluate the erbium excited state population it is necessary to quantify the amount of photons emitted by the studied samples. This is done by calibrating the number of photons emitted from Er^{3+} ions in Corning glass sample ([Er^{3+}]: 0.7×10^{20} at cm^{-3}), whose cross sections, thickness, radiative and total lifetime are known.

The total photon flux emitted by the sample can be then related to the number of Er^{3+} found in the excited state by the following relationship:

$$\Phi_{em} = \frac{N_2 V}{\tau_{rad}} \tag{4}$$

where τ_{rad} is the radiative lifetime estimated to be 16 ms, which accounts also for the material refractive index of the matrix, and V is the actual excited volume.

Fig. 4 presents the first excited state population (sample A) as a function of $\sigma_{exc}\Phi$. The solid line shows the result of the fitting by Eq. (2). Thus, it has been possible to extract the number of Er^{3+} coupled to the Si-nc, which coincides with the extrapolated value of N_2 at high photon fluxes. The absolute value of $3.6\times10^{19}\,cm^{-3}$ determined through this procedure turns to be about 23% of the optically active Er^{3+} content. The value of the optically active Er^{3+} content has been determined to be about half of the total Er^{3+} content by means of measurements under 980 nm pump excitation, which is resonant with an Er^{3+} transition and is not absorbed by Si-nc.

As a confirmation of the extracted value for the coupled Er^{3+} content we have also done pump and probe measurements under non-resonant pumping (476 nm). As it has been reported elsewhere Error! Reference source not found., we have been able to obtain an internal gain value as high as 1 dB cm^{-1}. The fact that about 4 dB cm^{-1} of absorption losses were found Error! Reference source not found leads us to the same conclusion, i.e., we are actually inverting about 25% of the optically active Er^{3+} content.

3.4. Auger back transfer to Si-nc

It has been reported [12] that two transfer processes govern the 1.54 μm emission:

(a) one fast (ns) process through which about 50% of the Er^{3+} population is indirectly excited. This is followed by a fast (ns) Auger back-transfer mechanism from Er^{3+} to Si-nc that quenches the Er emission;
(b) one slow (μs) process through which it is possible to excite only few percents of the Er^{3+} population and that is the prevailing mechanism in continuous wave regime.

We have performed ultra-fast time resolved IR photoluminescence measurements ($\lambda_{pump}=355$ nm, repetition rate = 10 Hz, pump pulse duration = 6 ns) to study the fast dynamics of the optical transitions related to Er^{3+} in our samples. As it can be seen in the inset of Fig. 5, we also demonstrate the existence of two processes in the 1.54 μm decay: (i) one fast (ns, rise and decay) and (ii) one slow (μs, rise). However, by spectrally resolving the two contributions, we note that the fast decay is observed at wavelengths different from the typical Er^{3+} transition. Fig. 5 shows the spectrally resolved time integrated emission of the fast (first 200 ns) and the slow (from 200 ns to 2 μs) contributions. Since the spectral dependence of the fast mechanism differs from that of Er^{3+}, we suggest that is not associated to Er^{3+} emission. On the other hand, the slow mechanism follows the Er^{3+} emission spectra, showing both the 980 nm and the 1.54 μm transitions. It is worth noting that the intensity of the 980 nm transition is stronger than the 1.54 μm

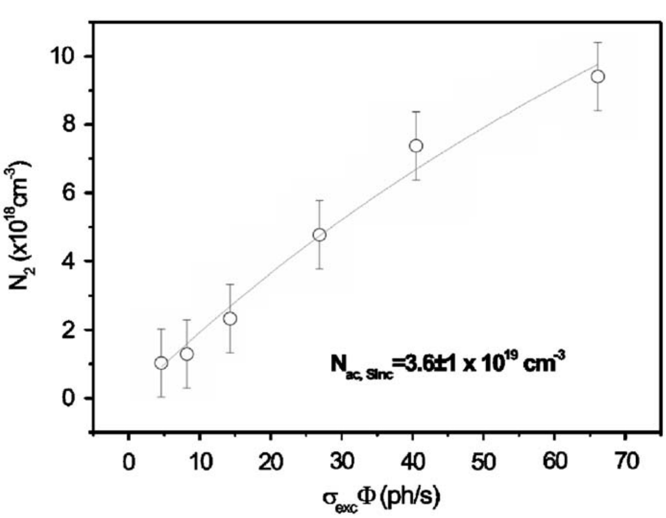

Fig. 4. First excited state population as a function of the product $\sigma_{eff}\Phi$. The fitting curve using Eq. (2) is also shown (solid line).

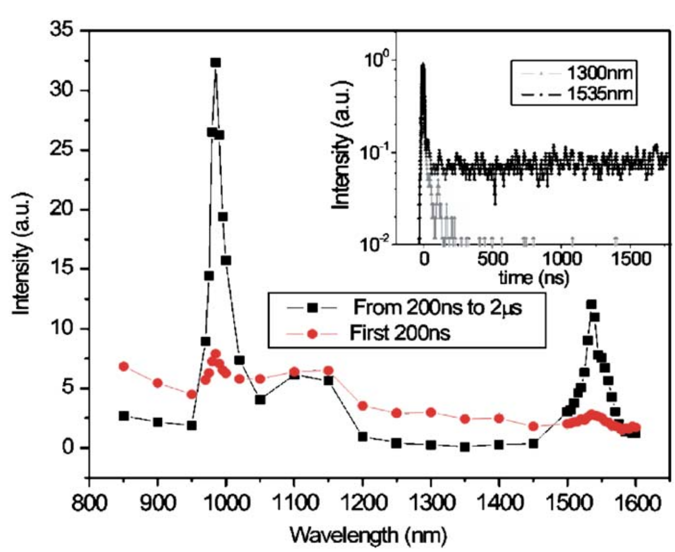

Fig. 5. Inset: fast time resolved PL signal for 1300 nm (grey) and 1535 nm (black). The spectral analysis obtained by integrating the first 200 ns (red circles) of the decay and from 200 ns to 2 μs (black squares) are shown in the main panel.

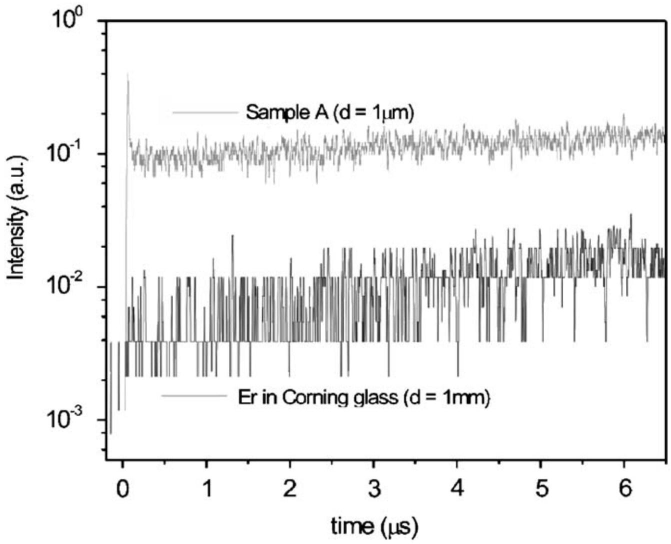

Fig. 6. Fast time resolved PL signal for 1535 nm for a Corning reference sample (black) and for sample A (grey) under the same pumping conditions.

one since its total lifetime is much shorter. The contribution at 1.1 μm is due to the silicon substrate.

We have also measured samples with the same Si-nc composition as sample A but without Er^{3+} codoping. In these samples, only a fast component in the IR region is observed. This fast component has a very similar spectral dependence as the one observed in sample A, although about three times more intense. It is thus likely that the fast component is not related to the Er^{3+} presence but it is simply due to the recombination of defect centers either in the silica matrix or at the interface of the Si-nc. From these results, it is possible to conclude that there is no sign of fast Auger back-transfer mechanisms in sample A and, therefore, Auger back transfer is not an issue in optimised samples.

As a confirmation of the indirect excitation of our samples under these pumping conditions, we have also measured a reference sample in which Er^{3+} is embedded in a Corning glass matrix, i.e. without the presence of Si-nc. The Er^{3+} concentration in both samples is roughly the same, but the thickness of the Corning sample is 1000 times larger. As it can be seen in Fig. 6 the signal from sample A is 10 times higher than the reference sample, even though we have not normalised the PL signal by the sample thickness. This implies that the excitation process in sample A is much faster, i.e. the effective excitation cross section at 355 nm is several orders of magnitude higher than the direct one. It is also worth noting that in the reference sample measurement there is no sign of a fast process.

4. Conclusions

We have reported on a set of reactive magnetron co-sputtering grown SiO_2 doped with Si-nc and Er^{3+} ions samples. By following a systematic procedure of material optimisation of the material, we have achieved 23% of the optically active Er^{3+} population efficiently coupled to Si-nc. This is about one order of magnitude higher than what obtained in previous works, and it has been obtained by reducing cooperative up-conversion and carrier absorption effects to negligible values and by increasing the total lifetime up to 5.5 ms. Moreover we have demonstrated that Auger back transfer is not present in our samples.

Thus we think, contrary to what was commonly believed, that the major, if not the only, constraining factor in achieving 100% Er^{3+} excitation is the limited interaction distance between Si-nc and Er^{3+} ions. This could be overcome by carefully placing the Er^{3+} in the close vicinity of Si-nc.

Acknowledgements

The authors would like to thank the financial support by EC through the LANCER Project (FP6-IST 033574) and in particular C.J. Oton and W. Loh (ORC, University of Southampton, UK) for the waveguide processing.

References

[1] P.G. Kik, A. Polman, in: L. Pavesi, et al. (Eds.), Towards the First Silicon Laser, NATO Science Series II, vol. 93, Kluwer, Dordrecht, 2003, p. 383.
[2] A.J. Kenyon, P.F. Trwoga, M. Federighi, C.W. Pitt, J. Phys. Condens. Matter 6 (1994) L319.
[3] M. Fujii, M. Yoshida, Y. Kanzawa, S. Hayashi, K. Yamamoto, Appl. Phys. Lett. 71 (1997) 1198.
[4] G. Franzò, V. Vinciguerra, F. Priolo, Appl. Phys. A A69 (1999) 3.
[5] J.H. Shin, S.-Y. Seo, S. Kim, S.G. Bishop, Appl. Phys. Lett. 76 (2000) 1999.
[6] P.G. Kik, M.L. Brongersma, A. Polman, Appl. Phys. Lett. 76 (2000) 2325.
[7] A. Pitanti, D. Navarro-Urrios, R. Guider, N. Daldosso, F. Gourbilleau, L. Khomenkova, R. Rizk, L. Pavesi, Proc. SPIE 6996 (2008) 699619.
[8] M. Wojdak, M. Klik, M. Forcales, O.B. Gusev, T. Gregorkiewicz, D. Pacifici, G. Franzò, F. Priolo, F. Iacona, Phys. Rev. B 69 (2004) 233315.
[9] P.G. Kik, A. Polman, J. Appl. Phys. 88 (2000) 1992.
[10] B. Garrido, C. García, S.-Y. Seo, P. Pellegrino, D. Navarro-Urrios, N. Daldosso, L. Pavesi, F. Gourbilleau, R. Rizk, Phys. Rev. B 76 (2007) 245308.
[11] D. Navarro-Urrios, N. Daldosso, C. García, P. Pellegrino, B. Garrido, F. Gourbilleau, R. Rizk, L. Pavesi, Jpn. J. Appl. Phys. 46 (10A) (2007) 6626.
[12] I. Izeddin, A.S. Moskalenko, I.N. Yassievich, M. Fujii, T. Gregorkiewicz, Phys. Rev. Lett. 97 (2006) 207401.
[13] D. Timmerman, I. Izeddin, P. Stallinga, I.N. Yassievich, T. Gregorkiewicz, Nat. Photonics 2 (2008) 105.
[14] F. Gourbilleau, C. Dufour, M. Levalois, J. Vicens, R. Rizk, C. Sada, F. Enrichi, G. Battaglin, J. Appl. Phys. 94 (2003) 3869.
[15] N. Daldosso, D. Navarro-Urrios, M. Merchiorri, C. Garcia, P. Pellegrino, B. Garrido, C. Sada, G. Battaglin, F. Gourbilleau, R. Rizk, L. Pavesi, IIIE J. Select. Topics. Quantum Electron. 12 (2006) 1607.
[16] D. Navarro-Urrios, A. Pitanti, N. Daldosso, F. Gourbilleau, R. Rizk, G. Pucker, L. Pavesi, Appl. Phys. Lett. 92 (2008) 051101.